MIT Open Access Articles

ADAM9 inhibition increases membrane activity of ADAM10 and controls #-secretase processing of amyloid precursor protein

ADAM9 INHIBITION INCREASES MEMBRANE ACTIVITY OF ADAM10 AND CONTROLS α–SECRETASE PROCESSING OF AMYLOID PRECURSOR PROTEIN

Marcia L. Moss[1], Gary Powell[2], Miles A. Miller[3], Qi Bin[4], Qing-Xiang Amy Sang[4], Bart De Strooper[5], Ina Tesseur[5], Stefan F. Lichtenthaler[6], Mara Taverna[6], Julia Li Zhong[7], Colin Dingwall[8], Taheera Ferdous[8], Uwe Schlomann[8], Pei Zhou[9], Linda Griffith[3], Douglas Lauffenberger[3], Robert Petrovich[2], and Jörg W. Bartsch[8,10]

From BioZyme Inc, 1513 Old White Oak Church Road, Apex, NC 27523[1]; NIEHS, 111 TW Alexander Dr. RTP, NC 27709, USA[2]; Department of Biological Engineering, Massachusetts Institute of Technology, Cambridge, MA 02139, USA[3]; Department of Chemistry & Biochemistry, Florida State University, Tallahassee, FL 32306-4390, USA[4]; Center for Human Genetics, Catholic University Leuven, 3000 Leuven, Belgium[5]; DZNE-German Center for Neurodegenerative Diseases, Munich, 80336 Munich, Germany[6]; College of Bioengineering, Chongqing University, Chongqing, 400044, China[7]; King's College London, Institute of Pharmacy, 150 Stamford Street, London, SE1 9NH, United Kingdom[8]; Department of Biochemistry, Duke University Medical Center, Durham, NC 27710 USA[9]; Department of Neurosurgery, Marburg University, University Hospital, Baldingerstr., 35053 Marburg, Germany[10].
Running head: ADAM9 affects cellular ADAM10 activity

Address correspondence to: Jörg W. Bartsch, Department of Neurosurgery, University Hospital, Baldingerstr., 35033 Marburg, Germany; Tel.: +49 6421 58-66753; FAX: +49 6421 58-66795; Email: jbartsch@med.uni-marburg.de

Capsule:
Background: Raising ADAM10 alpha-secretase activity has been considered as an attractive therapeutic option in Alzheimer's disease.
Results: Administration of prodomain of ADAM9 (ProA9) prevents ADAM10 shedding and increases membrane alpha secretase activity in a neuronal cell line.
Conclusion: Use of ProA9 is a mean to modulate cellular ADAM10 activity
Significance: ProA9 can be used *in vivo* to increase ADAM10 alpha secretase activity.

Prodomains of ADAM metallopeptidases can act as highly specific intra- and intermolecular inhibitors of ADAM catalytic activity. The mouse ADAM9 prodomain (proA9; amino acid 24-204), expressed and characterized from *E. coli*, is a competitive inhibitor of human ADAM9 catalytic/disintegrin domain with an overall inhibition constant of 280±34nM and high specificity towards ADAM9. In SY5Y neuroblastoma cells over-expressing amyloid precursor protein (APP), proA9 treatment reduces the amount of endogenous ADAM10 enzyme in the media whilst increasing membrane-bound ADAM10 as shown both by Western and activity assays with selective fluorescent peptide substrates using proteolytic activity matrix analysis (PrAMA). An increase in membrane-bound ADAM10 generates higher levels of soluble amyloid precursor protein alpha (sAPPα) in the media, whereas sAPPβ levels are decreased, demonstrating that inhibition of ADAM9 increases α-secretase activity on the cell membrane. Quantification of physiological ADAM10 substrates by a proteomic approach revealed that substrates such as epidermal growth factor (EGF), HER2, osteoactivin, and CD40-Ligand are increased in the media of BT474 breast tumor cells that were incubated with proA9, demonstrating that the regulation of ADAM10 by ADAM9 applies for many ADAM10 substrates. Taken together, our results demonstrate that ADAM10 activity is regulated by inhibition of ADAM9 and this regulation may be used to control shedding of APP by enhancing α-secretase activity, a key regulatory step in the aetiology of Alzheimer's disease.

1

Members of the ADAM (a disintegrant and metalloproteinase) family of proteinases function as sheddases by cleaving type I and type II integral single membrane proteins to generate soluble forms of these proteins(1,2). In addition to their catalytic and disintegrin domains, ADAM family members contain a prodomain that is required for expression, folding, and efficient transport of the proteinase(3). ADAM prodomains are efficient and highly specific inhibitors for their cognate ADAM proteases and even when proteolytically cleaved from their nascent polypeptides they can still serve as intermolecular inhibitors of their respective ADAM proteins(4,5). ADAM proteinases have functions in the etiologies of a variety of diseases and conditions. ADAM17 and 10, for example are known sheddases for over 40 different type I and II integral membrane proteins(6,7) and improper regulation of their catalytic activities is implicated in neurological diseases (8,9), carcinogenesis(10-12), and inflammatory conditions(13-18). In particular, the cleavage of Amyloid Precursor protein at the alpha secretase site is considered as instrumental in prevention of AD by favoring the non-amyloidogenic pathway(19). In neurons, ADAM10 has been demonstrated to be essential for the alpha secretase step of APP processing(20). Therefore means to control α-secretase levels are of therapeutic relevance in AD.

Understanding the hierarchy of ADAM proteinases could aid in determining broader biological mechanisms and reveals an additional level of ADAM regulation. For example, Cisse et al., demonstrated using transfection experiments that ADAM10 alpha secretase activity in mouse embryonic fibroblasts (MEFs) and a neuronal cell line, could be increased by ADAM9 overexpression, possibly by affecting the shedding or release of ADAM10 from the membrane of cells(21). Recently, Tousseyn et al. provided direct evidence that ADAM9 and ADAM15 process ADAM10 leaving behind an intracellular cytoplasmic domain ICD (22) with a potential function in regulating transcription of genes in the cell nucleus. This type of cleavage event is known as regulated intramembrane proteolysis or "RIP"(23). However, the physiological consequences of this cleavage step have remained elusive. A specific inhibitor of ADAM9 could be used to elucidate the physiological consequence of ADAM10 shedding, i.e. to investigate a possible regulation of ADAM10 dependent shedding events.

Typically, forced expression of ADAM family members in MEFs derived from knockout mice, and siRNA mediated silencing have been used as tools to validate the role of a particular disintegrin metalloproteinase in shedding events. We have chosen to use specific inhibitors in order to understand how modulation of only the enzyme's catalytic activity affects cellular processing as with pharmaceutical agents, activities oftentimes are regulated while the gene product remains intact. To date, the only available specific inhibitors of ADAM family members are small molecules described by Incyte(24,25), and protein therapeutics using modified tissue inhibitor of metalloproteinases(26), the prodomains' of ADAM17 and 10(4,5), and an antibody to ADAM17(27). Therefore, studies were undertaken to express, refold, purify, and examine a prodomain construct based on ADAM9 to easily achieve the highest degree of specificity for ADAM9 inhibition. A number of parameters were varied to obtain prodomain in milligram quantities that had refolded properly as assessed by inhibition studies with ADAM9. We demonstrate that the prodomain is a specific inhibitor of ADAM9 and show that ADAM9 regulates the cellular activity of ADAM10. Furthermore, proA9 was also used as a tool to demonstrate that specific inhibition of endogenous ADAM9 catalysis increases shedding of ADAM10 substrates in cellular assays.

Experimental Procedures
Materials
Human recombinant ADAM9, ADAM8, ADAM10, ADAM12 and ADAM17 proteases containing the catalytic/disintegrin domains, respectively, were obtained from R&D Systems (Minneapolis, MN). All oligonucleotides for PCR were synthesised from IDT DNA (Coralville, IA).

Methods
Cloning of ADAM9 cDNA- A DNA fragment containing ADAM9 prodomain (24-204) was cloned into a modified PET vector at the *Nde1*, *BamH1* restriction sites. The modified PET vector

encodes His6 between *NdeI* and *BamHI* sites to produce a protein with a N-terminal His-tag. DNA primers were: N-His (24-204), 5' primer, GGA GCC CAT ATG CCA GTC CTC GAG GCC GGG CGA, 3' primer, GGA GCC GGA TCC TTA TCT GCG CAG CTG AGT GAC ; N-His (24-204).

Expression and Purification of soluble Prodomain-The construct was transformed into *E. coli* strain BL21(DE3)STAR (Invitrogen, Carlsbad, CA). For a typical sample preparation, bacteria were grown in 4 x 1 litre of luria broth (LB) at 37ºC until the OD_{600} reached 0.4. The culture was incubated at 20ºC for 30 min before adding IPTG (1 mM) to induce protein expression. Cells were harvested after 16 hours by spinning at 4ºC for 30 min at 4000 rpm in a Sorvall JA 10 rotor. The supernatant was removed and pellets were either stored at -70ºC or used directly.

Cell pellets were lysed in 30 ml of buffer containing 50 mM phosphate, pH 8.0, 10 mM imidazole, 0.05% β-mercaptoethanol, and 300 mM NaCl at 4 ºC containing cell lytic (Sigma-Aldrich) (3 ml of a 10x concentrated solution). Lysed bacteria were sonicated to shear the DNA and RNA, and then polyethyleneimine was added to 0.1% to precipitate the DNA. Samples were centrifuged at 13,000 rpm for 30 minutes. The cleared supernatant was applied to 1 ml of TALON resin (Clontech, Mountain View, CA) pre-equilibrated with lysis buffer without cell lysate. After two 5 ml washes with lysis buffer and 50 mM phosphate, pH 8.0 containing 20 mM imidazole, 0.05% β-mercaptoethanol, and 300 mM NaCl, the protein was eluted with a solution containing 50 mM phosphate, pH 8.0, 150 mM imidazole, 0.05% β-mercaptoethanol, and 300 mM NaCl. The eluted protein was concentrated using an Amicon ultra filtration device (molecular weight cutoff 10 kDa) from Millipore (Billerica, MA) and further purified with a Sephacryl-S200 column (320 ml) on an Akta FPLC system at a flow rate of 1 ml/min. FPLC buffers contained 25 mM Tris, pH 8.0, 100mM NaCl and 0.05% β-mercaptoethanol. Fractions containing protein were concentrated and passed through an Endotrap blue column from Profos to remove endotoxin and then stored as 10% glycerol stocks at -80 ºC.

Expression, Refolding, and Purification of insoluble Prodomain- Colonies of freshly transformed ArcticExpress™ (Agilent Technologies, Santa Clara, CA) or BL21(DE3) (Invitrogen, Carlsbad, CA) were used in all refolding and expression experiments. Cells from a 1L overnight culture grown in LB containing ampicillin and gentamycin, were centrifuged at 5,500 x g and re-suspended in 50 mL LB broth. Twenty-five millilitres of this suspension was used to inoculate one litre of LB containing ampicillin. For the ArcticExpress conditions, cultures were incubated at 10°C with shaking for 2 hours, induced by adding IPTG to 0.2 mM, and grown for an additional 20 hours. Cells were harvested by centrifugation for 15 min at 5,500 x g at 4°C.
Inclusion bodies containing proA9 were isolated from cells lysed in 5 volumes of Bug Buster Master Mix (Novagen), 0.5mg/ml of lysozyme (Sigma-Aldrich), 5 mM $MgCl_2$ and 5 mM NaATP, containing Complete™ EDTA-free proteinase inhibitors (Roche Diagnostics), per gram of cell paste. The lysis suspension was incubated 30 min at room temperature with gentle agitation, and centrifuged for 30 min at 16,000 x g at 4°C to collect the inclusion bodies. Purification of inclusion bodies was accomplished by washing twice vs. 5 vol of 0.1x Bug Buster Master Mix and 2 times vs. 5 volumes of water. The resulting pellets were resuspended in water or 50mM Tris-Cl, pH 8.0 and stored frozen at -80°C.
Refolding conditions were established using the HiPER-FOLD™ Starter kit from Barofold.

Using the best refolding conditions determined above, inclusion bodies were added to buffer containing 50mM CHES, pH9 and 5mM TCEP, and then placed under pressure in a Barofold apparatus for 24hr at room temperature. Soluble protein after the pressure was released, was purified further by passage through 10 ml of Ni-NTA resin (Qiagen, Valencia, CA) followed by washes of 10 and 20 mM imidazole, and elution with 250 mM imidazole in buffers that contained 4mM TCEP, 50 mM NaPi, pH 8, and 300 mM NaCl. The eluted protein was concentrated to less than 5 ml using an Amicon ultra filtration device (molecular weight cutoff 10 kDa) from Millipore (Billerica, MA) and further purified with a Sephadex-16/60 column (120 ml) on an Akta FPLC system at a flow rate of 1 ml/min. FPLC

3

buffers contained 25 mM Tris, pH 8.0, 100 mM NaCl and 4 mM TCEP. Fractions containing protein were concentrated, passed through an Endotrap Blue column from Hyglos/Profos, and stored as 10% glycerol stocks at -80°C. In some experiments, proA9 was refolded from inclusion bodies from BL21(DE3) purified via a Ni column and then dialyzed against 25mM CHES, pH9, 100mM NaCl and 0.035% beta mercaptoethanol or passed through a Sephadex- 16/60 column using the same buffer conditions. In addition, proA9 was sometimes refolded from urea after purification with Ni-NTA agarose, and then further purified via a Sephadex 16/60 column.

Inhibition assays- Fluorescence intensities were measured every 2 minutes at excitation and emission wavelengths of 485 and 530 nm, respectively at room temperature in black coated 96 well plates using a top to bottom Fluoroskan II fluorometer. Activity of TACE catalytic-disintegrin, ADAM8, ADAM12 and ADAM10 catalytic/disintegrin recombinant proteins was monitored as previously described using the fluorescent substrate PEPDab005 (28). Inhibition assays were done using up to 8.4 μM proA9. ADAM9 activity was assayed using the fluorescent substrate PEPDab010 (29) in 70μl of buffer with 5μl of proA9 (75-8000 nM final) or buffer control. For each proA9 concentration, a well containing only proA9 and substrate were used to correct for fluorescence fluctuations due to the prodomain itself. ADAM9 was provided as a 0.1 μg/μl stock solution, which was diluted 1:50 from which 8 μl was added to start the reaction. The functional purity of ADAM9 was confirmed by using hydroxamate inhibitors and the determination of IC_{50}s which were compared to literature values(29).

Measurement of ADAM10 activity in the media and in membrane fractions- SY5Y neuroblastoma cells were cultured in duplicate using a 6 well plate for 24 hr in serum free media with proA9 (5μM) or a buffer control. Media was removed and spun to remove cell fragments, and set aside for assaying. Cells were washed with PBS and then scraped from the plate and resuspended in a 1.5ml tube in a cold solution of 0.25M sucrose, 50mM Tris, pH8, and a protease inhibitor cocktail from Roche Diagnostics. Cells were broken via

pipetting up and down, and the suspension was spun at 13,000 x g to pellet the membranes which were resuspended and washed with sucrose buffer. After pelleting, membranes were resuspended in 200μl of sucrose buffer per well of cells. Protein concentrations were determined using the BioRad BPA assay.

The media and membrane suspension were tested for ADAM10 activity by using the Proteolytic Activity Matrix Analysis (PrAMA) technique developed by Miller (30) using substrates PEPDab005, PEPDab010, PEPDab008, PEPDab013, PEPDab014 that varied in their specificities towards different ADAM family members and MMPs. Briefly, 12.5 μM substrate concentrations in ADAM buffer, 60μl, were incubated with either 20 μl of media or 10μl of resuspended membranes. Fluorescence units vs. time were monitored with a Fluostar BMG Optima using excitation and emission wavelengths of 485 and 530 nM respectively. Data were analyzed by taking the initial velocities and fitting to a matrix developed previously using the PrAMA technique.

Calculation of K_i values
The fractional inhibitor activity, I_f, was calculated by dividing the initial velocity from the FU vs. time graph obtained with inhibitor, v_i, by the initial velocity without inhibitor, v_o. All inhibition assays were performed at room temperature and the data fit to the following equation using Sigma Plot software:

$$I_f = \frac{I}{(I + K_i app)} \quad (1)$$

I_f is fractional inhibition, I is the inhibitor concentration and K_{iapp} is the inhibitor concentration that gives 50% inhibition.

Mechanism of Inhibition- ADAM9 was diluted 1:500 in buffer 25 mM Tris pH 8, 6 x 10^{-4} % Brij-35 and 35 μl was added to a 96 well plate. Various concentrations of prodomain (2 μl volume) in 25 mM Tris-Cl, pH 8, 100 mM NaCl, 10% glycerol, 4 mM TCEP, and 10 mM $CaCl_2$ was added to the enzyme and preincubation was carried out for 15 min. Then 33 μl of substrate (5-100 μM) of PEPDab010 was added and fluorescence intensities were measured with

4

excitation at 485 nm and emission at 530 nm. The final concentration of prodomain ranged from 75-4000 nM. Fluorescence vs. time was plotted and slopes were derived from straight line fits of initial velocities. The reciprocals of the velocities were plotted vs. the reciprocals of substrate squared since the normal Lineweaver-Burk plot gave curved lines. The initial velocities vs. substrate concentrations were fit as a family of curves to several allosteric models. The data fit best to a pure competitive model as described in equation 2 where binding of inhibitor prevents substrate from binding to both sites.

$$v = V * (\frac{S}{K_s} + \frac{S^2}{K_s^2}) / (1 + \frac{2S}{K_s} + \frac{S^2}{K_s^2} + \frac{I}{K_i}) \qquad (2)$$

In this equation, v is the velocity obtained from the fluorescence units vs time plot, V is the maximum velocity, S is the substrate concentration, I is the inhibitor concentration, K_s is the dissociation constant for substrate binding to enzyme, and K_i is the inhibition constant.

Cell culture- SH-SY5Y-APP$_{swe}$ neuroblastoma cells expressing APP with the Swedish mutation (APP$_{swe}$: APP^{K595N}, APP^{M596L}) were cultured in DMEM supplemented with 10 % FBS, 2 mM Glutamin, and 400 μg/ml G418. For ADAM10 and APP shedding analyses, cells were maintained in serum-free medium for 6 and 12 hours. Cell culture supernatants were analysed by western blotting and ELISA after concentrating using Vivaspin columns (Generon, UK) with an exclusion range of 20 kD.

Western Blotting- For Western blot sample preparations, cell supernatants were concentrated and mixed with 5x SDS sample buffer (50% glycerol, 10% SDS, 100 mM β-mercaptoethanol, 0.05% bromophenol blue in 250 mM Tris-HCl, pH 6.8), boiled for 10 min and loaded onto 7.5% SDS-PAGE for soluble APP detection. After gel runs, the proteins were blotted onto nitrocellulose transfer membranes (Protran BA79, 0.1 mm pore size, Schleicher & Schuell, Dassel, Germany) by tank blotting. After control staining with 0.1% Ponceau S solution and blocking for 2 h with 5% skim milk in TBS containing 0.1% Tween-20, proteins were analysed by immunostaining using

antibodies described under materials in the given concentrations.

ELISAs- Concentrations of sAPPβ were determined using the MSD sAPPß Assay and MSD Ab triplex assay as described by the manufacturer (Meso Scale Discovery, Gaithersburg, MD, USA). Concentrations of sAPPα were measured using a biotinylated-antibody (clone 14D6) with the same specificity as the 4B4 [15]. The streptavidin pre-coated 96-well plates (MSD, L15SA-1/L11SA-1) were blocked with blocking solution for 30 minutes, washed 3 times with Tris Wash Buffer and coated with the biotinylated antibody 14D6 for 1 hour. After washing 3 times, the wells were incubated with 25 ml of standards or samples and 25 ml of the anti-rabbit 5313 antibody for 2 hours. The wells were washed 3 times and incubated with 25 ml of MSD Sulfo-Tag goat-anti-rabbit-antibody (MSD, R32AB-5) as detection antibody. The wells were washed 3 times and incubated with the MSD Read Buffer T and the MSD plates were measured on the MDS Sector Image 600 plate reader. The raw data were measured as electrochemiluminescence signal detected by photodetectors.

Statistical analysis- Data were presented as mean values ± standard deviation. The student's t test was applied for data analysis. P values <0.05 were considered significant.

Peptide Microarray experiments- BT474 breast tumor cells were obtained from ATCC and were grown in RPMI media containing 10% Fetal Bovine Serum. The cells were seeded at $1x10^6$ cells/ml plated in either 96 or 6 well plates. After overnight incubation cells were placed in Minimum Essential Media (MEM) without serum. Prodomain of ADAM9, ADAM10 or a buffer control were added to the media after filter sterilization with a 0.22 μm filter. The final concentration of glycerol was adjusted to 1%. After 24 hr, media was collected and frozen. The frozen media analyzed by RayBiotech in an L series 507 microarray. Data were normalized to both positive and negative controls that were run alongside samples. Each run represents averages of triplicate values after normalization. Ratios of control vs. treated were determined for two separate runs. Data were presented as mean

5

values. Values between 0.8 and 1.4 for an average of two runs indicates no change in factor levels while a value below 0.8 means a decrease of factor in the media for the treated cells.

Results

Generation and characterization of ADAM9 prodomain- A bacterial expression construct for the prodomain of ADAM9 (proA9) was generated excluding the N-terminal hydrophobic signal sequence region and terminated at the furin cleavage site (aa 24-204 of mADAM9). A construct encoding a C-terminal His-tagged protein rendered a completely insoluble protein (data not shown), so that the N-terminal construct was used in all studies.

Since the yield of recombinant protein was low (< 50 μg/l), refolding of proA9 was done from inclusion bodies. Once refolded, samples were analyzed for protein content by SDS PAGE and for inhibitory potency against ADAM9 to assess if the prodomain had refolded properly (Table 1 and Fig. 1A). The optimal refolding conditions proved to be 50mM CHES, pH 9 with 5mM TCEP without arginine.

ProA9 purified from the insoluble fraction after refolding, had identical properties to the proA9 obtained from the soluble fraction (Figure 1B,C). Using this proA9 preparation, inhibition studies against several recombinant ADAM proteases were carried out to evaluate specificity. Recombinant proA9 is an efficient inhibitor of human ADAM9, with an apparent inhibition constant, $K_{i(app)}$, of 280 ± 34nM (Figure 2A; Table 2). ADAM8 and 12 are weakly inhibited by proA9 with approximate apparent K_is in the micromolar range (>1μM and >6μM respectively). Recombinant ADAM10 and ADAM17/TACE proteases were not inhibited by proA9 even at concentrations of ≥ 8 μM (Table 1). Given these parameters, a low μM concentration of proA9 can be used in cell-based assays to inhibit ADAM9 activity.

Mechanism of Inhibition- ProA9 was tested to determine the mode of inhibition for human ADAM9. A typical Lineweaver-Burk plot, where the substrate was varied as a function of inhibitor concentration, gave curved lines for the reciprocal plot. Thus a $1/v$ vs. $1/[S^2]$ plot was used and gave a

good fit with varying slopes but the intercepts remaining the same (Figure 2B). This indicated that proA9 is a competitive inhibitor of ADAM9. This analysis also indicated that ADAM9 has at least two binding sites for the fluorescent substrate. The velocities vs. substrate at varying inhibitor values were fit as a family of curves to the pure competitive inhibitor model. The K_i, calculated with this method was 240 ± 110 nM and the binding constant, K_s for substrate was 37 ± 9μM. The K_i is in close agreement to what was found for the apparent inhibition constant, $K_i$app, calculated from the inhibition data eq (1).

ProA9 inhibits ADAM10 shedding and increases alpha secretase activity on the cell membrane- In an earlier report, shedding of ADAM10 by ADAMs 9 and 15 was described, but the physiological consequences of this process remain elusive(21,22). We used the proA9 as a specific inhibitor to address this question. To provide direct evidence for ADAM9 regulating ADAM10 activity, SH-SY5Y neuroblastoma cells over-expressing APP were treated with proA9 at concentrations of 1 and 5 μM and the extent of soluble ADAM10 was determined by Western blotting using an antibody directed against the MP domain of ADAM10 (Fig. 3A). ADAM9 inhibition by proA9 resulted in reduced release of soluble ADAM10 (30 ± 4% for 1 μM, 15 ± 5% for 5 μM) in the media. Furthermore, a method developed previously, termed Proteolytic Activity Matrix Analysis (PrAMA)(30), was used to quantify the amount of proteolytically active ADAM10 in the media. PrAMA employs a panel of synthetic FRET-based polypeptide protease substrates to record a quantitative signature of cleavage rates for a given biological sample. Prior knowledge of individual MMP/ADAM cleavage specificity profiles measured with purified enzymes allows PrAMA to decipher specific enzyme (e.g., ADAM10) activities from observed cleavage signatures. In this work, we used five different proteinase substrates as described in M&M that vary in their specificity for ADAMs and MMPs to infer the activities of MMP9, ADAM10, and ADAM17. PrAMA analysis confirmed a decrease in the amount of ADAM10 activity in media from SY5Y cells with proA9 treatment (Fig 3B), while no significant change in

6

MMP9 or ADAM17 activity was observed (data not shown).   These results demonstrate that inhibition of ADAM9 leads to a significant reduction of ADAM10 release and confirm previous findings that ADAM9 is a processing enzyme for ADAM10(21,22,31).

We next tested whether this reduction caused an increase in the membrane associated activity of ADAM10. Western analysis and FRET assays of the membrane fraction were accomplished and analyzed by PrAMA. The amount of ADAM10 as measured by both of these techniques indicated an increase in the cellular fraction after proA9 treatment of the SY5Y cells (Figure 3C). As with analysis of the media, PrAMA did not detect significant changes in ADAM17 activity upon proA9 treatment. Since ADAM10 activity was increased on the membrane of cells given a specific inhibitor of ADAM9, the release of amyloid precursor protein (APP), a physiological substrate for ADAM10, was quantified by ELISA from SY5Y cells to determine if soluble APP levels increased in media from proA9 treated cells (Figure 4 A-C).

Western analysis of whole cell lysate and supernatant from SY5Y cells after proA9 treatment indicated similar amounts of APP (Figure 4A). However, when media was collected after 6 and 12 hour treatments with proA9 or a buffer control and the amounts of sAPPα and sAPPβ were analyzed via a multiplex ELISA, a dose dependent increase in sAPPα and corresponding decrease in sAPPβ was detected, indicating that the alpha secretase activity of ADAM10 can be regulated by specific inhibition of ADAM9 (Figure 4B,C).

Peptide microarray screening- Having shown that ADAM9 regulates ADAM shedding activity, a protein array analysis was performed to obtain a more general screen on the regulation of ADAM9 and ADAM10 activity in cancer cells. The Ray Biotech L series protein array was chosen because it had been successfully used in other published assays to quantify protein levels in samples from cell media or biological fluids (32). In the RayBiotech patented approach, media samples, either treated or buffer control, was biotin labeled and incubated on a glass chip printed with 507

different antibodies. Briefly BT474 cells were treated with 5μM proA9. As a comparison to proA9 inhibition, proA10 was used as a specific inhibitor of ADAM10 dependent shedding events.

Using this method, three different groups of proteins can be classified (Table 3): an increase in the media of physiological substrates for ADAM10 after proA9 treatment (proA10 treatment resulted in a reduction of the same substrates), a decrease in the media of factors after proA9 but not proA10 inhibition, and an attenuation of factors found in the media after either proA9 or proA10 treatment.

In the first group, endogenous shedding of known ADAM10 substrates such as Her2, osteoactivin, CD40-Ligand, and EGF were all downregulated by proA10 and upregulated by proA9 addition to the BT474 cells. In contrast, novel factors possibly shed by ADAM9 and not by ADAM10 were also found such as MAC-1, glucocorticoid-induced tumour necrosis factor receptor (GITR), platelet derived growth factor alpha (PDGF-Rα), and transforming growth factor-alpha (TGF-α). Several proteins decreased in the media from cells treated with either inhibitor such as neuropilin2, lipopolysaccharide binding protein (LBP), and OX40-ligand. In addition, tumor necrosis factor receptor 1 (TNF-R1) and tumor necrosis factor-alpha (TNF)/amphiregulin (AR), physiological substrates for ADAM8 (33) and ADAM17 (34-36) respectively, were not affected by proA9 or proA10 treatments, indicating that the inhibitors are quite selective in their actions (data not shown).

Discussion

With respect to the selectivity of proA9, the observed IC_{50} for inhibition of ADAM8 is slightly higher than 1μM (see table 2), so the K_i difference is about 5-fold. However it is likely that some inhibition of ADAM8 may occur at 5μM proA9 concentration, even though in BT474 cells, the presence of both L-selectin and TNF-R1 in the media, two substrates for ADAM8 is not affected by proA9 treatment. This could be due to very low ADAM8 levels in BT474 cells that was confirmed by RNA analysis and by a PrAMA experiment where the substrate specific for ADAM8 (PEPDab013) is only slightly processed in both membrane and media samples,

7

even though other less selective substrates with the same k_{cat}/K_m for ADAM8 are processed very well (data not shown).

Since ADAM10 has been described as the essential α-secretase in neurons, the control of neuronal ADAM10 activity has crucial importance in the aetiology of AD (20) and attempts to raise cellular ADAM10 levels have been considered as potential therapeutic strategies in AD (19). We found that specific proA9 mediated inhibition of ADAM9 catalytic activity in SY5Y neuroblastoma cells regulates ADAM10 activity on the cell membrane by preventing its proteolytic release. Because the amount of membrane bound ADAM10 increases when its shedding is reduced, we postulate that the enzyme's cleavage activity would correspondingly be increased. In accordance with these findings, proA9 inhibition of ADAM9, a principal sheddase for ADAM10, leads to an increase in the alpha secretase activity for APP in cell based assays, increasing the extracellular levels of sAPPα, arguing for an inhibition of ADAM9 to favor a non-amyloidogenic pathway. Since ADAM9 is dispensable *in vivo* as shown by ADAM9 deficient mice(37), this therapeutic strategy seems to be feasible.

In previous studies loss and gain of function assays were performed in transfected cells and demonstrated that ADAM9 indirectly increases the amount of sAPPα likely through cleavage of ADAM10. Our findings demonstrate that an immediate reduction in soluble ADAM10 by inhibition of ADAM9 catalysis increases ADAM10 processing of APP at the alpha cleavage site. This complements more long-term experiments that require longer periods to constitute a complex interplay of ADAM proteins after knockdown (21) or over-expression of ADAM9 in the presence of siRNA for ADAM10 (31). In addition, we demonstrate the effect of endogenous inhibition of ADAM9 rather than a reduction in its activity after transfection.

Further proof that ADAM9 inhibition leads to an increase in membrane ADAM10 activity arises from results with the BT474 tumor cells where increased levels of proteins for proven substrates of ADAM10 were found in the media from proA9 treated cells. Of 507 different factors that can be detected in media samples by the microarray approach, only a handful are secreted at reduced levels and several are type I or II membrane proteins capable of serving as substrates for ADAM9. These factors range from receptors to growth factors. The mechanism by which proA9 specifically reduces type I and II integral membrane protein levels in the media is likely due to its inhibition of ADAM9 catalytic activity as it is a competitive inhibitor. In contrast, proA10 treatment affects ADAM10 dependent shedding events (over 100 factors are reduced in the media from BT474 treated cells; data not shown) but has no effect in parallel assays on the newly identified potential substrates for ADAM9. These results indicate that generally specific inhibition of ADAM9 controls membrane ADAM10 activity which could be of general *in vivo* relevance.

References

1. Edwards, D. R., Handsley, M. M., and Pennington, C. J. (2008) *Mol Aspects Med* **29**, 258-289

2. Saftig, P., and Reiss, K. *Eur J Cell Biol* **90**, 527-535

3. Leonard, J. D., Lin, F., and Milla, M. E. (2005) *Biochem J* **387**, 797-805

4. Gonzales, P. E., Solomon, A., Miller, A. B., Leesnitzer, M. A., Sagi, I., and Milla, M. E. (2004) *J Biol Chem* **279**, 31638-31645

5. Moss, M. L., Bomar, M., Liu, Q., Sage, H., Dempsey, P., Lenhart, P. M., Gillispie, P. A., Stoeck, A., Wildeboer, D., Bartsch, J. W., Palmisano, R., and Zhou, P. (2007) *J Biol Chem* **282**, 35712-35721

6. Crawford, H. C., Dempsey, P. J., Brown, G., Adam, L., and Moss, M. L. (2009) *Curr Pharm Des* **15**, 2288-2299

7. Arribas, J., and Esselens, C. (2009) *Curr Pharm Des* **15**, 2319-2335

8. Postina, R., Schroeder, A., Dewachter, I., Bohl, J., Schmitt, U., Kojro, E., Prinzen, C., Endres, K., Hiemke, C., Blessing, M., Flamez, P., Dequenne, A., Godaux, E., van Leuven, F., and Fahrenholz, F. (2004) *J Clin Invest* **113**, 1456-1464

9. Pan, D., and Rubin, G. M. (1997) *Cell* **90**, 271-280

10. Turner, S. L., Blair-Zajdel, M. E., and Bunning, R. A. (2009) *Br J Biomed Sci* **66**, 117-128

11. Murphy, G. (2008) *Nat Rev Cancer* **8**, 929-941

12. Zhou, B. B., Fridman, J. S., Liu, X., Friedman, S. M., Newton, R. C., and Scherle, P. A. (2005) *Expert Opin Investig Drugs* **14**, 591-606

13. Weskamp, G., Ford, J. W., Sturgill, J., Martin, S., Docherty, A. J., Swendeman, S., Broadway, N., Hartmann, D., Saftig, P., Umland, S., Sehara-Fujisawa, A., Black, R. A., Ludwig, A., Becherer, J. D., Conrad, D. H., and Blobel, C. P. (2006) *Nat Immunol* **7**, 1293-1298

14. Lemieux, G. A., Blumenkron, F., Yeung, N., Zhou, P., Williams, J., Grammer, A. C., Petrovich, R., Lipsky, P. E., Moss, M. L., and Werb, Z. (2007) *J Biol Chem* **282**, 14836-14844

15. Naus, S., Blanchet, M. R., Gossens, K., Zaph, C., Bartsch, J. W., McNagny, K. M., and Ziltener, H. J. *Am J Respir Crit Care Med* **181**, 1318-1328

16. Koller, G., Schlomann, U., Golfi, P., Ferdous, T., Naus, S., and Bartsch, J. W. (2009) *Curr Pharm Des* **15**, 2272-2281

17. Hass, M. R., Sato, C., Kopan, R., and Zhao, G. (2009) *Semin Cell Dev Biol* **20**, 201-210

18. Moss, M. L., Sklair-Tavron, L., and Nudelman, R. (2008) *Nat Clin Pract Rheumatol* **4**, 300-309

19. Fahrenholz, F. (2007) *Curr Alzheimer Res* **4**, 412-417

20. Kuhn, P. H., Wang, H., Dislich, B., Colombo, A., Zeitschel, U., Ellwart, J. W., Kremmer, E., Rossner, S., and Lichtenthaler, S. F. *EMBO J* **29**, 3020-3032

21. Cisse, M. A., Sunyach, C., Lefranc-Jullien, S., Postina, R., Vincent, B., and Checler, F. (2005) *J Biol Chem* **280**, 40624-40631

22. Tousseyn, T., Thathiah, A., Jorissen, E., Raemaekers, T., Konietzko, U., Reiss, K., Maes, E., Snellinx, A., Serneels, L., Nyabi, O., Annaert, W., Saftig, P., Hartmann, D., and De Strooper, B. (2009) *J Biol Chem* **284**, 11738-11747

9

23. De Strooper, B., Annaert, W., Cupers, P., Saftig, P., Craessaerts, K., Mumm, J. S., Schroeter, E. H., Schrijvers, V., Wolfe, M. S., Ray, W. J., Goate, A., and Kopan, R. (1999) *Nature* **398**, 518-522

24. Liu, X., Fridman, J. S., Wang, Q., Caulder, E., Yang, G., Covington, M., Liu, C., Marando, C., Zhuo, J., Li, Y., Yao, W., Vaddi, K., Newton, R. C., Scherle, P. A., and Friedman, S. M. (2006) *Cancer Biol Ther* **5**, 648-656

25. Zhou, B. B., Peyton, M., He, B., Liu, C., Girard, L., Caudler, E., Lo, Y., Baribaud, F., Mikami, I., Reguart, N., Yang, G., Li, Y., Yao, W., Vaddi, K., Gazdar, A. F., Friedman, S. M., Jablons, D. M., Newton, R. C., Fridman, J. S., Minna, J. D., and Scherle, P. A. (2006) *Cancer Cell* **10**, 39-50

26. Kveiborg, M., Jacobsen, J., Lee, M. H., Nagase, H., Wewer, U. M., and Murphy, G. *Biochem J* **430**, 79-86

27. Tape, C. J., Willems, S. H., Dombernowsky, S. L., Stanley, P. L., Fogarasi, M., Ouwehand, W., McCafferty, J., and Murphy, G. *Proc Natl Acad Sci U S A* **108**, 5578-5583

28. Moss, M. L., and Rasmussen, F. H. (2007) *Anal Biochem* **366**, 144-148

29. Moss, M. L., Rasmussen, F. H., Nudelman, R., Dempsey, P. J., and Williams, J. (2010) *Comb Chem High Throughput Screen* **13**, 358-365

30. Miller, M. A., Barkal, L., Jeng, K., Herrlich, A., Moss, M., Griffith, L. G., and Lauffenburger, D. A. (2011) *Integr Biol (Camb)* **3**, 422-438

31. Taylor, D. R., Parkin, E. T., Cocklin, S. L., Ault, J. R., Ashcroft, A. E., Turner, A. J., and Hooper, N. M. (2009) *J Biol Chem* **284**, 22590-22600

32. Turtinen, L. W., Bremer, L. A., Prall, D. N., Schwartzhoff, J., and Hartsel, S. C. (2005) *Immunopharmacol Immunotoxicol* **27**, 85-93

33. Bartsch, J. W., Wildeboer, D., Koller, G., Naus, S., Rittger, A., Moss, M. L., Minai, Y., and Jockusch, H. (2011) *J Neurosci* **30**, 12210-12218

34. Black, R. A., Rauch, C. T., Kozlosky, C. J., Peschon, J. J., Slack, J. L., Wolfson, M. F., Castner, B. J., Stocking, K. L., Reddy, P., Srinivasan, S., Nelson, N., Boiani, N., Schooley, K. A., Gerhart, M., Davis, R., Fitzner, J. N., Johnson, R. S., Paxton, R. J., March, C. J., and Cerretti, D. P. (1997) *Nature* **385**, 729-733

35. Moss, M. L., Jin, S. L., Milla, M. E., Bickett, D. M., Burkhart, W., Carter, H. L., Chen, W. J., Clay, W. C., Didsbury, J. R., Hassler, D., Hoffman, C. R., Kost, T. A., Lambert, M. H., Leesnitzer, M. A., McCauley, P., McGeehan, G., Mitchell, J., Moyer, M., Pahel, G., Rocque, W., Overton, L. K., Schoenen, F., Seaton, T., Su, J. L., Becherer, J. D., and et al. (1997) *Nature* **385**, 733-736

36. Sunnarborg, S. W., Hinkle, C. L., Stevenson, M., Russell, W. E., Raska, C. S., Peschon, J. J., Castner, B. J., Gerhart, M. J., Paxton, R. J., Black, R. A., and Lee, D. C. (2002) *J Biol Chem* **277**, 12838-12845

37. Weskamp, G., Cai, H., Brodie, T. A., Higashyama, S., Manova, K., Ludwig, T., and Blobel, C. P. (2002) *Mol Cell Biol* **22**, 1537-1544

38. Amour, A., Knight, C. G., Webster, A., Slocombe, P. M., Stephens, P. E., Knauper, V., Docherty, A. J., and Murphy, G. (2000) *FEBS Lett* **473**, 275-279

39. Rose, A. A., Annis, M. G., Dong, Z., Pepin, F., Hallett, M., Park, M., and Siegel, P. M.(2010) *PLoS One* **5**, e12093

40. Rose, A. A., and Siegel, P. M. (2007) *Breast Cancer Res* **9**, 403

10

41. Sahin, U., Weskamp, G., Kelly, K., Zhou, H. M., Higashiyama, S., Peschon, J., Hartmann, D., Saftig, P., and Blobel, C. P. (2004) *J Cell Biol* **164**, 769-779

42. Nocentini, G., Giunchi, L., Ronchetti, S., Krausz, L. T., Bartoli, A., Moraca, R., Migliorati, G., and Riccardi, C. (1997) *Proc Natl Acad Sci U S A* **94**, 6216-6221

43. Hirahashi, J., Hishikawa, K., Kaname, S., Tsuboi, N., Wang, Y., Simon, D. I., Stavrakis, G., Shimosawa, T., Xiao, L., Nagahama, Y., Suzuki, K., Fujita, T., and Mayadas, T. N. (2009) *Circulation* **120**, 1255-1265

44. Leon, F., Contractor, N., Fuss, I., Marth, T., Lahey, E., Iwaki, S., la Sala, A., Hoffmann, V., Strober, W., and Kelsall, B. L. (2006) *J Immunol* **177**, 6974-6982

45. Morrison, T. E., Simmons, J. D., and Heise, M. T. (2008) *J Virol* **82**, 11263-11272

46. Matei, D., Emerson, R. E., Lai, Y. C., Baldridge, L. A., Rao, J., Yiannoutsos, C., and Donner, D. D. (2006) *Oncogene* **25**, 2060-2069

47. Lee, D. C., Luetteke, N. C., and Petch, L. A. (1992) *Cancer Treat Res* **63**, 233-254

48. Gray, P. W., Flaggs, G., Leong, S. R., Gumina, R. J., Weiss, J., Ooi, C. E., and Elsbach, P. (1989) *J Biol Chem* **264**, 9505-9509

49. Zhao, H., Bernardo, M. M., Osenkowski, P., Sohail, A., Pei, D., Nagase, H., Kashiwagi, M., Soloway, P. D., DeClerck, Y. A., and Fridman, R. (2004) *J Biol Chem* **279**, 8592-8601

50. Nasarre, C., Koncina, E., Labourdette, G., Cremel, G., Roussel, G., Aunis, D., and Bagnard, D. (2009) *Cell Adh Migr* **3**, 383-389

51. Fassold, A., Falk, W., Anders, S., Hirsch, T., Mirsky, V. M., and Straub, R. H. (2009) *Arthritis Rheum* **60**, 2892-2901

52. Geretti, E., van Meeteren, L. A., Shimizu, A., Dudley, A. C., Claesson-Welsh, L., and Klagsbrun, M. (2010) *Mol Cancer Res*

Acknowledgements

Footnotes

[1] The Abbreviations used are: aa, amino acid; ADAM, a disintegrin and metalloproteinase; CM, conditioned media; Dabcyl, 4-(4-Dimethylaminophenylazo)benzoyl; DMSO, dimethyl sulfoxide; EGF, epidermal growth factor; EGFR, epidermal growth factor receptor; Fam, 5-carboxyfluorescein; GITR, glucocorticoid-induced tumour necrosis factor receptor; IPTG, isopropyl-β-D-thiogalactopyranoside; LBP, lipopolysaccharide binding protein; mEF, mouse embryonic fibroblast; PDGF-Rα, platelet derived growth factor alpha; PEPDab005, Dabcyl-Leu-Ala-Gln-Ala-Homophenyl-Arg-Ser-Lys(Fam)- NH$_2$; PEPDab008, Dabcyl-Pro-Cyclohexyl-Gly-Cys(Me)-His-Ala-Lys(Fam)-NH$_2$; PEPDab010, Dabcyl-Ser-Pro-Leu-Ala-Gln-Val-Arg-Ser-Ser-Lys(Fam)- NH$_2$; PEPDab013, Dabcyl-His-Gly-Asp-Gln-Met-Ala-Gln-Lys-Ser-Lys(Fam)-NH$_2$; PEPDab014, Dabcyl-Glu-HisAla-Asp-Leu-Leu-Ala-Val-Val-Ala-Lys(Fam)-NH$_2$; ProA9, prodomain of ADAM9; ProA10, prodomain of ADAM10; TACE, tumor necrosis factor-alpha converting enzyme; TCEP, tris(2-

carboxyethyl)phosphine; TNF-R1, p55 tumor necrosis factor receptor 1; TNF, tumor necrosis factor; TGF-α, transforming growth factor-alpha.

Figure Legends

Figure 1: Purification and characterization of proA9 from inclusion bodies. **(A)** SDS-polyacrylamide gel of proA9 refolded in a variety of buffers. The band corresponding to the proA9 recombinant protein. ProA9 was prepared under different pH and redox conditions shown in table 1; R, arginine added to buffers; Redox, glutathione oxidized and reduced mixture; **(B)** SDS-polyacrylamide gel of proA9 purified from the soluble fraction by Talon resin chromatography and Superdex 75 fractionation. **(C)** SDS-polyacrylamide gel of proA9 purified from inclusion bodies. Lane 1, insoluble fraction following pressure-mediated refolding of proA9 inclusion body protein; lane 2, soluble fraction; lane 3, Ni-chelating chromatography pool; lane 4, Sephacryl 200 pool; lane 5, proA9 following endotoxin removal.

Figure 2: **(A)** Plot of v_i/v_o against concentration of proA9 (I) in nM. The IC50 is plotted a dotted line. **(B)** Lineweaver-Burk plot of $1/v$ vs $1/S^2$ in the presence of various concentrations of proA9. Symbols: ■ 600nM, △ 300nM, ○ 150nM, ◆ 75nM, ✳ 0nM.

Figure 3: Inhibition of ADAM10 shedding by proA9 in SY5Y cells and regulation of ADAM10 alpha secretase activity. **(A)** Western blot of soluble ADAM10 in supernatants of SY5Y cells. Cells were incubated for 24 hours untreated ("ctrl"), with buffer control (corresponding to the proA9 volume of 5 μM), with 500 nM BB-94, 500 ng hTIMP-1 or proA9 in concentrations of 1 ("ProA9 (1)") and 5 ("proA9 (5)") μM, respectively. Supernatants were concentrated and precipitated with TCA. Samples were resuspended in Laemmli buffer and separated on 10% polyacrylamide gels. Blots were incubated with anti-ADAM10 detecting the extracellular portion of ADAM10. A 55kD band represents the soluble form of ADAM10, containing the MP and parts of the disintegrin domain, in agreement with the data published earlier (22). **(B)** Membrane-associated ("M") and soluble ADAM10 ("S") activities in the absence ("ctrl") and presence of 5 μM proA9 ("proA9") were analysed by PrAMA as described in the M&M section. Fluorescence values are given as mean values ± SD from 3 independent experiments. *, p<0.05. **(C)** Detection of membrane-associated ADAM10 in SY5Y cells. Cells treated with buffer ("ctrl") or 5 μM proA9 ("proA9") were lysed and membranes were isolated as described in M&M. After protein concentrations were determined, identical concentrations of membrane preparations were analyzed by western blotting using anti-ADAM10 antibody.

Figure 4: Effect of proA9 on APP shedding in SH-SY5Y cells overexpressing APP(swe). **(A)** Western blot analysis of APP in whole cell lysates ("WCL") and in supernatants ("SN"). Note that in the supernatant, APP α and β is detected; **(B)** and **(C)**, MSD ELISAs (Meso Scale Discovery) were used to determine the concentrations of soluble APP-alpha (sAPPα; **B**) and soluble APP-beta (sAPPβ; **C**). The electric signal measured with the ELISA was converted into concentrations in [pg/ml] by using calibration curves for each individual analysis. The values given are derived from 2 sets of quadruplets (n=8) and are given as mean ± SD. Statistical significance was determined using Student's t-test and values are provided as highly significant (***, p<0.001, **, <0.01, *, p<0.05).

12

Lane #	Sample ID	% Inhibition
1	pH8	75
2	pH9	97
3	pH6 +R	22
4	pH7 +R	75
5	pH8 +R	89
6	pH9 +R	84
7	pH9 +Redox	60
8	pH8 +R+Redox	42
9	pH7 +0.5xR	69
10	pH7 +0.25xR	71
11	pH7 +0.1xR	77
12	pH8 +0.5xR	93
13	pH8 +0.25xR	0

Table 1: Corresponding inhibitory activity of ADAM9 using a fixed volume of buffer containing proA9 from different refolding conditions. Refolding conditions for proA9 varied in pH values, presence of arginine (R), and/or glutathione oxidized and reduced mixture ("Redox"). Note that identical sample numbers 1-13 are shown in lanes figure 1A.

Rec. Protease	ProA9 K_i [nM]
ADAM8	> 1000
ADAM9	280± 34
ADAM10	> 8000
ADAM12	>6000
ADAM17	> 8000

Table 2: Inhibition of protease activity by proA9 for different recombinant ADAM proteins. ProA9 was incubated with the human recombinant ADAM proteins indicated and the amount of inhibition was determined by fluorometric assay as described in M&M section.

Factor	Description	Disease association	Ratio pA9/buffer control	Ratio pA10/buffer control	Ref.
Group I					
ErbB2	Receptor tyrosine kinase	Cancer	2.5± 1.0	0.6±0.1	(24)
CD40-L		Inflammation	2.0±0.4	0.3±0.1	(38)
Osteoactivin	Transmembrane glycoprotein NMB (GPNMB)	Cancer	2.5±0.5	0.60±0.1	(39,40)
EGF	Epidermal Growth Factor	Cancer	3.3±1.2	0.6±0.1	(41)
GroupII					
GITR ligand	Glucocorticoid-induced tumour necrosis factor receptor (GITR) ligand	Inflammatory activation of macrophages	0.3±0.1	0.9±0.1	(42)
MAC-1	Complement receptor (CR3)	Inflammatory diseases, viral infection	0.5±0.1	1.4±0.1	(43-45)
PDGF-Rα	Tyrosine kinase receptor for platelet derived growth factor alpha	Cancer	0.5±0.1	1.1±0.3	(46)
TGF-α	Epidermal growth factor ligand family member	Cancer	0.2±0	1.4±0.2	(47)
GroupIII					
LBP	Binds Lipopoly-saccaride/ Acute phase protein	localized defense to Gram negative bacteria	0.3±0.1	0.5±0.2	(48)
MT3-MMP	Membrane type 3-Matrix metalloproteinase	Cancer	0.3±0.1	<0.1	(49)
Neuropilin-2	Receptor for semaphorins and VEGF	Cancer	0.6±0.3	0.3±0.1	(50-52)

Table 3: Ratios of Type I and II integral membrane proteins in media after proA9 and proA10 treatment of BT474 cells. ProA9 (5μM) or ProA10 (23-213 wild type, 10μM) and corresponding buffer controls were incubated alongside with BT474 cells for 24 hr in serum free conditions. Media were collected and analyzed by the RayBiotech 507 L series microarray. Data represents the average ratio from two independent runs done in triplicate.
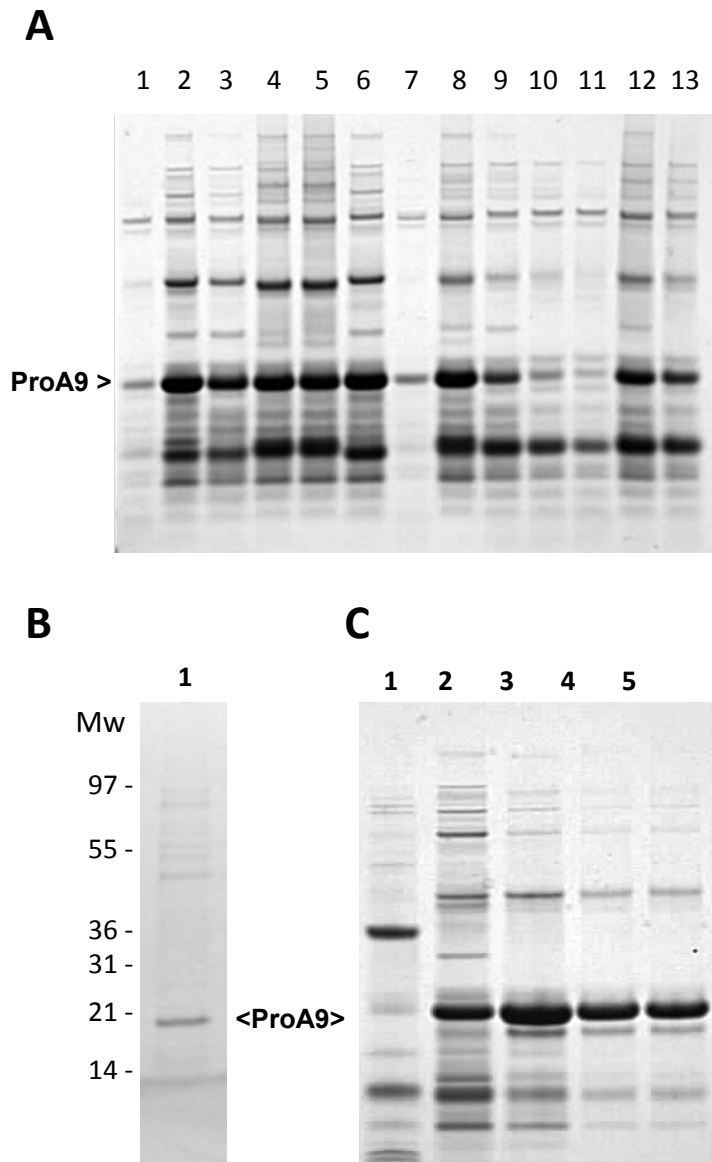
A

1 2 3 4 5 6 7 8 9 10 11 12 13

ProA9 >

B
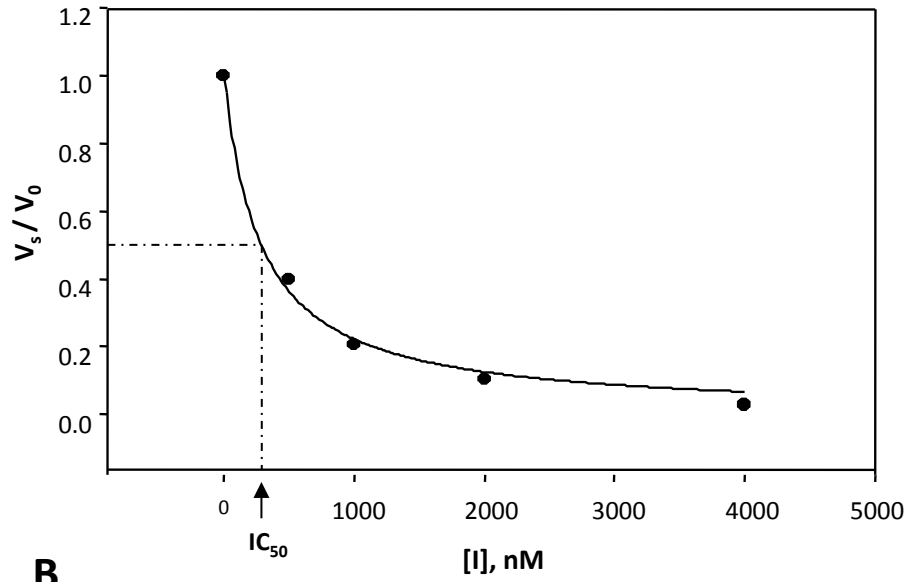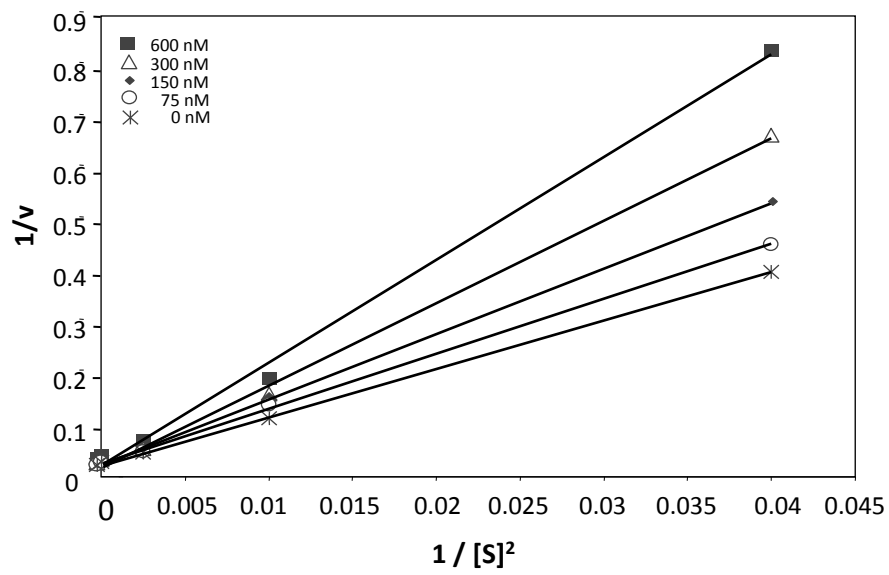
1

Mw

97 -

55 -

36 -
31 -

21 - <ProA9>

14 -

C
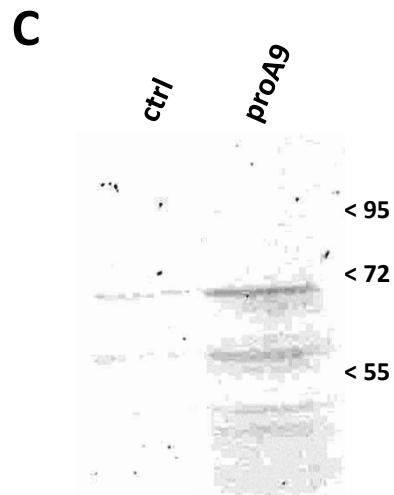
1 2 3 4 5
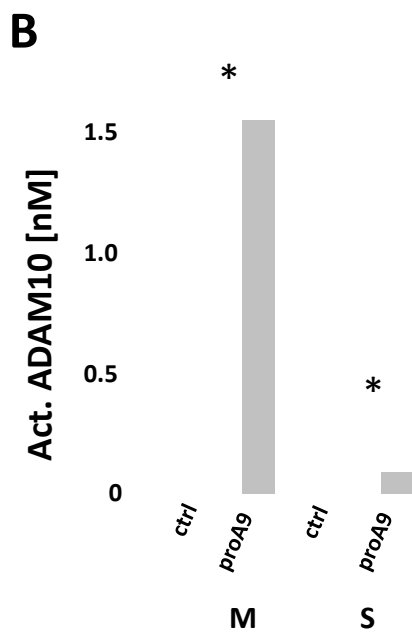
Figure 1 Moss et al.,

A

B

Figure 2, Moss et al.,

A

ctrl buffer BB-94 TIMP-1 proA9 (1) proA9 (5)

sA10 ▶

LC ▶

B

*

Act. ADAM10 [nM]

1.5

1.0

0.5

0

ctrl proA9 ctrl proA9

M   S

*

C

ctrl proA9

< 95

< 72

< 55

Figure 3 Moss et al.,

A

250 >
130 >
95 >
72 >
55 >
36 >

control   proA9 (5)   control   proA9 (5)

< sAPP

APP SN

< 55

APP WCL   β-tubulin

B

sAPPα

Conc. [pg/ml]

7000
6000
5000
4000
3000
2000
1000
0

***   ***   ***   ***

Ctrl   B   1   5   B   1   5
      6h   12h

C

sAPPβ

3500
3000
2500
2000
1500
1000
500
0

*   **

Ctrl   B   1   5   B   1   5
      6h   12h

Figure 4 Moss et al.,